

# **Detecting Interplay of Chirality, Water, and Interfaces for Elucidating Biological Functions**

Elsa C. Y. Yan,<sup>1\*</sup> Ethan A. Perets,<sup>1#</sup> Daniel Konstantinovsky,<sup>1, 2</sup> Sharon Hammes-Schiffer<sup>1</sup>

<sup>1</sup>Department of Chemistry, Yale University, New Haven, CT 06520, USA

<sup>2</sup>Department of Molecular Biophysics and Biochemistry, Yale University, New Haven, CT  
06520, USA

<sup>#</sup>Current Address: Department of Chemistry and Chemical Biology, Harvard University,  
Cambridge, MA 02138, USA

\*Corresponding authors

Email addresses: [elsa.yan@yale.edu](mailto:elsa.yan@yale.edu),

## Conspectus

Chemists have long been fascinated by chirality, water, and interfaces, making tremendous progress in each research area. However, the chemistry emerging from the interplay of chirality, water, and interfaces has been difficult to study due to technical challenges, creating a barrier to elucidating biological functions at interfaces. Most biopolymers (proteins, DNA, and RNA) fold into macroscopic chiral structures to perform biological functions. Their folding requires water, but water behaves differently at interfaces, where the bulk water hydrogen-bonding network terminates. A question arises as to how water molecules rearrange to minimize free energy at interfaces while stabilizing macroscopic folding of biopolymers to support biological function. This question is central to solving many research challenges, including the molecular origin of biological homochirality, folding and insertion of proteins into cell membranes, and design of heterogeneous biocatalysts. Researchers can resolve these challenges if they have theoretical tools to accurately predict molecular behaviors of water and biopolymers at various interfaces. However, developing such tools requires validation by experimental data. These experimental data are scarce because few physical methods can simultaneously distinguish chiral folding of the biopolymers, separate signals of interfaces from the overwhelming background of bulk solvent, and differentiate water in hydration shells of the polymers from water elsewhere.

We have recently illustrated these very capacities of chirality-sensitive vibrational sum frequency generation spectroscopy (chiral SFG). While chiral SFG theory dictates that the method is surface-specific under the condition of electronic non-resonance, we show the method can distinguish chiral folding of proteins and DNA, and probe water structures in the first hydration shell of proteins at interfaces. Using amide I signals, we observe protein folding into  $\beta$ -sheets without background signals from  $\alpha$ -helices and disordered structures at interfaces, thereby demonstrating the effect of two-dimensional crowding on protein folding. Also, chiral SFG signals of C-H stretches are silent from single-stranded DNA, but prominent for canonical antiparallel duplexes as well as non-canonical parallel duplexes at interfaces, allowing for sensing DNA secondary structures and hybridization. In establishing chiral SFG for detecting protein hydration structures, we observe an  $\text{H}_2^{18}\text{O}$  isotopic shift that reveals water contribution to the chiral SFG spectra. Additionally, the phase of the O-H stretching bands flips when the protein chirality is switched from L to D. These experimental results agree with our simulated chiral SFG spectra of water hydrating the  $\beta$ -sheet protein at the vacuum-water interface. The simulations further reveal

that over 90% of the total chiral SFG signal comes from water in the first hydration shell. We conclude that the chiral SFG signals originate from achiral water molecules that assemble around the protein into a chiral supramolecular structure with chirality transferred from the protein. As water O-H stretches can reveal hydrogen-bonding interactions, chiral SFG shows promise in probing structures and dynamics of water-biopolymer interactions at interfaces. Altogether, our work has created an experimental and computational framework for chiral SFG to elucidate biological functions at interfaces, setting the stage for probing the intricate chemical interplay of chirality, water, and interfaces.

## Key References

- Liu, W.; Fu, L.; Wang, Z.; Sohrabpour, Z.; Li, X.; Liu, Y.; Wang, H.-F.; Yan, E. C. Y. Two dimensional crowding effects on protein folding at interfaces observed by chiral vibrational sum frequency generation spectroscopy.<sup>1</sup> *Physical Chemistry Chemical Physics* **2018**, *20*, 22421-22426. *Chiral SFG detects folding of the N-terminus of a zinc finger into  $\beta$ -sheets at the air-water interface using amide I signals without background from  $\alpha$ -helical and disordered structures, thereby illustrating the crowding effect in 2-dimensional space that inhibits folding of a zinc finger.*
- Perets, E. A.; Olesen, K. B.; Yan, E. C. Y. Chiral sum frequency generation spectroscopy detects double-helix DNA at interfaces. *Langmuir* **2022**, *38*, 5765-5778.<sup>2</sup> *Chiral SFG vibrational spectra of double-stranded and single-stranded DNA show chiral SFG is sensitive not to local chiral centers of chemical structures but to macroscopic chirality of DNA secondary structures at interfaces, allowing for label-free and background-free detection for DNA duplexes.*
- Perets, E. A.; Konstantinovsky, D.; Fu, L.; Chen, J.; Wang, H.-F.; Hammes-Schiffer, S.; Yan, E. C. Y. Mirror-image antiparallel  $\beta$ -sheets organize water molecules into superstructures of opposite chirality. *Proc. Natl. Acad. Sci.*, **2020**, *117*, 32902-32909.<sup>3</sup> *Heterodyne detection revealed the phase of the chiral SFG response of water switches signs when native (L-) protein is replaced by non-native (D-) protein, establishing that protein hydration structures can be chiral with their chirality imprinted from the proteins.*
- Konstantinovsky, D.; Perets, E. A.; Santiago, T.; Velarde, L.; Hammes-Schiffer, S.; Yan, E. C. Y. Detecting the first hydration shell structure around biomolecules at interfaces. *ACS Cent. Sci.* **2022**, *8*, 1404-1414.<sup>4</sup> *Simulations show chiral vibrational spectroscopy is sensitive to water molecules in the first hydration shell of a  $\beta$ -sheet protein at an interface. Analyzing the orientation of water dipoles around the protein explains this sensitivity based on symmetry-based chiral SFG theory.*

## Introduction

Chirality, water, and interfaces are linked to the origin of life.<sup>5</sup> While each has long been a subject of intense interest in chemistry, how they interact with one another at the molecular level has remained largely unexplored due to technical challenges that hinder elucidation of biological functions at interfaces. Biological functions are encoded at the molecular level in genomes and carried out by biopolymers, proteins, DNA, and RNA. These polymers are built by homochiral monomers, i.e., (L-) amino acids and (D-) nucleic acids, and fold into macroscopic chiral structures that are also homochiral.<sup>6, 7</sup> For example, (L-) proteins fold into right-handed but not left-handed  $\alpha$ -helices (Figure 1a). Correct folding of biopolymers is essential for their biological functions but requires the mediation of water.<sup>8</sup> Water has been a central research area in chemistry. Its extensive hydrogen-bonding networks (Figure 1b) generate many fascinating chemical and physical properties that support life processes,<sup>9</sup> including an enormous dielectric constant for modulating electrostatic interactions and a large specific heat capacity for regulating temperature. These types of properties can change drastically at an interface, where two media meet to create a boundary. Across the boundary, the asymmetric chemical environment aligns molecules (e.g., air-water, Figure 1c), manifesting new properties, such as catalyzing reactions that cannot take place in bulk solutions.

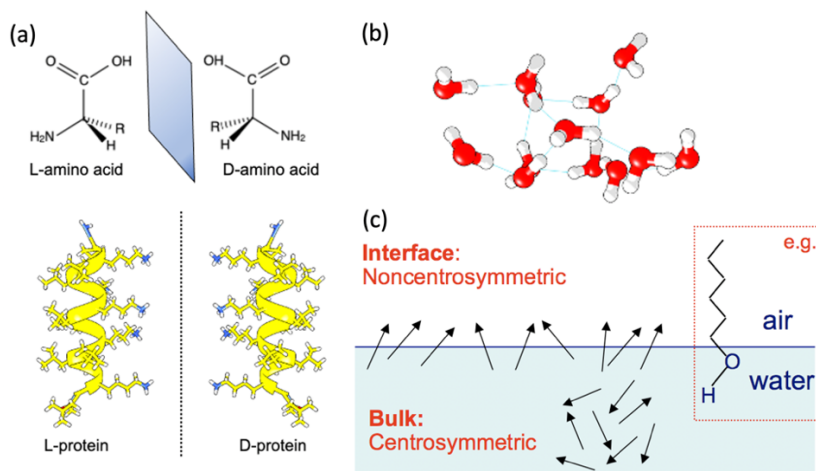


**Fig. 1. Chirality, water, and interfaces: three important research areas in chemistry.** (a) A native protein formed by (L-) amino acids folds into a right-handed  $\alpha$ -helix and its mirror-image non-native (D-) protein. (b) A hydrogen-bonding network in liquid water. (c) Asymmetric molecular environment at interfaces. Inset: a long-chain alcohol is oriented at the air-water interface.

Elucidating biological functions at interfaces requires fundamental understanding of how the asymmetric environment regulates water molecules in stabilizing correct folding of biopolymers. This is a complex question. One can grasp the complexity by imagining a biopolymer (e.g., protein) diving into water. Water molecules surrounding the polymer can stay in the bulk hydrogen-bonding network (Figure 1b) or break away from it to stabilize a particular fold of the biopolymer. Either case contributes to a delicate balance of free energy. Predicting such a balance to yield a hydrated three-dimensional structure of the biopolymer has been a grand research challenge in biophysics.<sup>8</sup> Now, the biopolymer moves to an interface, where the water hydrogen-bonding networks terminate suddenly.<sup>10-13</sup> A layer of complexity is then added as to how water molecules rearrange at the interface to minimize their free energy while stabilizing the folded structure of the biopolymer to support biological function. Answering this question is key to many research problems, such as searching for the molecular origin of homochirality in the biological world, understanding the molecular mechanism of protein folding and simultaneously inserting into cell membranes, designing biocompatible materials for industrial applications, and innovating biocatalysts for generating renewable energy.

Researchers can solve these problems if they can count on theoretical tools to predict structures and dynamics of biopolymers and water at various interfaces. Nonetheless, these theoretical tools need experimental benchmarks for validation. High-quality experimental benchmarks are limited due to a series of stringent demands on experimental methods. Ideally, the methods do not rely on readouts from molecular labels that can perturb water and biopolymers. They can operate under ambient conditions for *in situ* and real-time studies. They can also distinguish different chiral macroscopic folding of the biopolymers, such as protein  $\beta$ -sheet versus  $\alpha$ -helix. Moreover, they should have surface-selectivity in detecting molecules only at interfaces without the overwhelming background signals of bulk solution. Finally, they need to separate signals from water molecules in the hydration shell of the biopolymers from the vast population of water molecules elsewhere. These demands have posed a technical barrier in elucidating biological functions at interfaces.

Our recent work has shown that chirality-sensitive vibrational sum frequency generation (chiral SFG) spectroscopy can potentially overcome this technical barrier.<sup>1-4, 14</sup> Based on chiral SFG theory, the method is surface specific under the condition of electronic non-resonance.<sup>15-17</sup>

We show that chiral SFG can distinguish chiral folding of various secondary structures of proteins and DNA at interfaces.<sup>1, 2, 18-20</sup> Combining experiments and computations, we demonstrate that chiral SFG can detect water vibrational structures of the first hydration shell of a  $\beta$ -sheet protein at an interface.<sup>3, 4, 14, 21</sup> Our work has established an experimental and computational framework of chiral SFG to investigate structural and dynamical properties of water-biopolymer interactions at interfaces, introducing an approach to explore new chemistry emerging from the molecular interplay of chirality, water, and interfaces for elucidating biological functions.

## Selectivity to Interfaces

**Surface-selectivity.** Chiral SFG has been developed as a subtype of second-order vibrational sum frequency generation (SFG) spectroscopy, referred to as conventional SFG<sup>22-31</sup> or achiral SFG here. Studies of interfaces using SFG require two ultrafast laser beams, one in the visible frequency range ( $\omega_{\text{vis}}$ ) and one in the infrared frequency range ( $\omega_{\text{IR}}$ ). These two beams temporally and spatially overlap at an interface and generate second-order optical signals at the sum frequency ( $\omega_{\text{vis}} + \omega_{\text{IR}}$ ) (Figure 2a). Vibrational SFG keeps the frequency of the visible beam constant while varying the infrared frequency to resonate with vibrations of molecules at interfaces. Thus, SFG is a vibrational tool.

To differentiate conventional SFG and chiral SFG,<sup>15-17, 20, 32</sup> we need to understand the formulation of the SFG optical response in terms of second-order susceptibility ( $\chi^{(2)}$ ) and the physical meaning of  $\chi^{(2)}$ . An SFG experiment measures the SFG intensity ( $I_{\text{SFG}}$ ) or optical field ( $\mathbf{E}_{\text{SFG}}$ ) (Figure 2a). Any light intensity is the square of the magnitude of the optical field of electromagnetic radiation, and the optical field can be expressed using unit vector ( $\hat{\mathbf{x}}$ ,  $\hat{\mathbf{y}}$ , and  $\hat{\mathbf{z}}$ ) in laboratory coordinates (x, y, z) (Equation 1 and Figure 2a). Under the electric dipole approximation, the SFG optical field is related to the incident visible optical field ( $\mathbf{E}_{\text{vis}}$ ) and infrared optical field ( $\mathbf{E}_{\text{IR}}$ ) via the second-order susceptibility,  $\chi^{(2)}$ :

$$\mathbf{E}_{\text{SFG}} = E_{\text{SFG}}^x \hat{\mathbf{x}} + E_{\text{SFG}}^y \hat{\mathbf{y}} + E_{\text{SFG}}^z \hat{\mathbf{z}} \quad (1)$$

$$E_{\text{SFG}}^I \propto \sum_{JK} \chi_{IJK}^{(2)} E_{\text{vis}}^J E_{\text{IR}}^K \quad (2)$$

The second-order susceptibility ( $\chi^{(2)}$ ) is a third-rank tensor containing 27 elements,  $\chi_{IJK}^{(2)}$ , where the indices  $I$ ,  $J$ , and  $K$  indicate the direction of the three optical fields and can be equal to x, y, or z in the laboratory frame. For a particular vibrational normal mode, namely the  $q^{\text{th}}$  normal mode, each  $\chi^{(2)}$  element is an ensemble average of the molecular SFG response that is the hyperpolarizability ( $\beta$ ):

$$\chi_{IJK,q}^{(2)} \propto \sum_n \sum_{ijk} R_{Ii}^n R_{Jj}^n R_{Kk}^n \beta_{ijk,q}^n \quad (3)$$

where  $\beta_{ijk,q}^n$  are the hyperpolarizability tensor elements for the  $n^{\text{th}}$  moiety (such as a water molecule in a molecular system or an amide group in a protein);  $R_{Ii}^n$ ,  $R_{Jj}^n$ , and  $R_{Kk}^n$  are elements of the rotational transformation matrix projecting the SFG response from the molecular frame to the laboratory frame;  $I$ ,  $J$ ,  $K$  indicate directions in laboratory coordinates ( $x$ ,  $y$ ,  $z$ ); and  $i$ ,  $j$ , and  $k$  indicate directions in molecular coordinates ( $a$ ,  $b$ ,  $c$ ) with  $i$ ,  $j$ ,  $k$  = a, b, or c. Equation 3 describes a general case, where the hyperpolarizability ( $\beta$ ) for the  $q^{\text{th}}$  vibrational mode of each moiety being analyzed can be different due to local interactions and vibrational coupling. The  $\beta$  element for the  $n^{\text{th}}$  moiety is related to the Raman and infrared vibrational responses of the  $q^{\text{th}}$  vibrational normal mode:

$$\beta_{ijk,q}^n \propto \frac{\partial \alpha_{ij}^n}{\partial Q_q} \frac{\partial \mu_k^n}{\partial Q_q} \quad (4)$$

Where  $\partial \alpha_{ij}^n / \partial Q_q$  is the transition polarizability derivative (Raman) tensor and  $\partial \mu_k^n / \partial Q_q$  is the infrared transition dipole derivative with respect to the  $q^{\text{th}}$  normal mode coordinates ( $Q_q$ ). Thus, a vibrational mode must be both Raman active (i.e.,  $\partial \alpha_{ij}^n / \partial Q_q \neq 0$ ) and infrared active (i.e.,  $\partial \mu_k^n / \partial Q_q \neq 0$ ) in order to be SFG active. Hence, SFG can assess the microscopic vibrational response of molecules ( $\beta_{ijk,q}$ ) by measuring the macroscopic second-order susceptibility tensor elements ( $\chi_{IJK,q}^{(2)}$ ).

Chiral SFG is surface sensitive but only under the condition of *electronic non-resonance*. This condition is fulfilled when the visible beam used in an SFG experiment is at a frequency far from any electronic resonance of the molecular systems.<sup>15-17, 32</sup> Nonetheless, Belkin *et al.* reported chiral SFG signals from bulk pure chiral liquid even under the electronic non-resonance condition,<sup>33, 34</sup> and many researchers in the field of nonlinear spectroscopy had long considered chiral SFG to be lacking surface specificity until Simpson explained how chiral SFG signals arise

from the interface.<sup>15-17</sup> Under the condition of electronic non-resonance, Simpson considered a chiral interface with  $C_\infty$  symmetry and an achiral surface with  $C_{\infty v}$  symmetry (Figure 2b).<sup>15-17</sup> These two types of surfaces share common symmetry characteristics: (1) isotropic molecular arrangement on the surface plane and (2) anisotropic molecular arrangement across the interface (Figure 1c). These two characteristics lead to seven non-zero  $\chi^{(2)}$  elements, shown in blue in Figure 2b. Conventional SFG measures these non-zero elements and offer surface selectivity. A chiral surface, however, differs from an achiral surface in lacking reflection planes perpendicular to the interface. This lowering of symmetry results in six additional non-zero  $\chi^{(2)}$  elements (red, Figure 2b), which are orthogonal with the characteristics of  $\chi_{IJK}^{(2)} (I \neq J \neq K)$ . These orthogonal elements are zero for achiral interfaces ( $C_{\infty v}$ ) but non-zero for chiral interfaces ( $C_\infty$ ). They are measured in chiral SFG experiments.

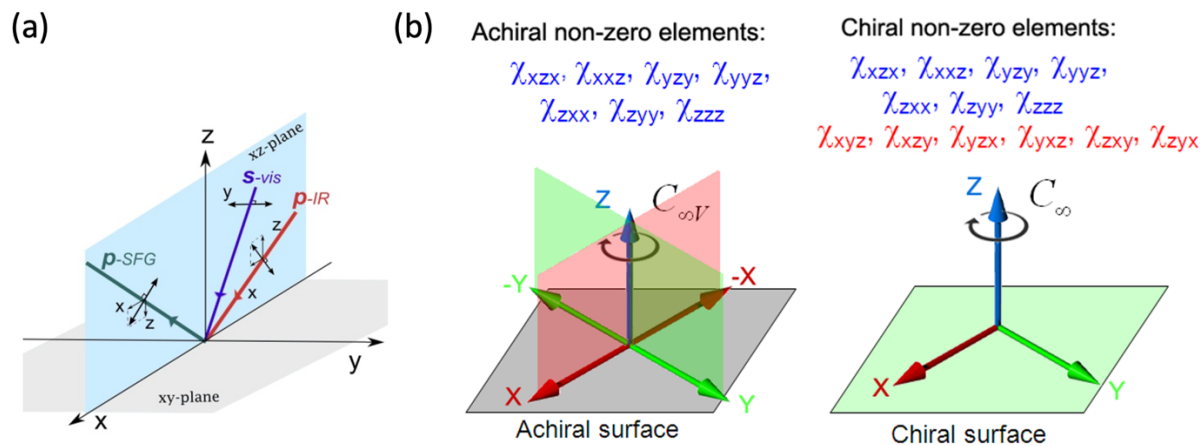


**Figure 2. Experimental and theoretical background of chiral SFG.** (a) An SFG experiment for studying interfaces is set up by overlapping a visible beam and an infrared beam at an interface and detecting SFG signals in the reflection geometry. The visible and infrared beams are often linearly polarized in *s*- or *p*-polarization, and the *s*- and *p*-components of the SFG signal can be isolated and measured. The setting of polarization can vary, allowing for measurements of individual or a subset of the 27 second-order susceptibility ( $\chi^{(2)}$ ) elements (equations 1 and 2). (b) An achiral interface has  $C_{\infty v}$  symmetry whereas a chiral interface has  $C_\infty$  symmetry. Group theory dictates that seven (blue) out of the 27 elements are non-zero for both achiral and chiral surfaces, but an additional six orthogonal  $\chi_{IJK}^{(2)} (I \neq J \neq K)$  elements (red) are non-zero only for a chiral interface. Under the condition of electronic non-resonance, the *psp* polarization setting shown in (a) can be used to measure the orthogonal  $\chi_{zyx}^{(2)}$  element in chiral SFG experiments. Adapted with permission from ref 20. Copyright 2014 American Chemical Society.

Further derivations using equations (3) and (4), as detailed elsewhere,<sup>15-17, 20</sup> showed that the orthogonal  $\chi^{(2)}$  elements, which are the source of the chiral SFG signal from a chiral interface ( $C_\infty$ ), originate from the *symmetric* components of the Raman polarization tensor ( $\alpha$ ). As Belkin *et al.*<sup>33</sup> pointed out, however, the chiral SFG signals from bulk media are contributed only by the *antisymmetric* tensor components. Under the condition of electronic non-resonance, the antisymmetric components of the Raman tensor are orders of magnitude smaller than the symmetric components.<sup>35</sup> Therefore, the bulk chiral SFG signals due to the antisymmetric components are negligible relative to the surface chiral SFG signal due to symmetric components. Hence, any significant chiral SFG signal measured from a molecular system with an anisotropic chiral interface in contact with an isotropic chiral bulk medium must come from the chiral interface with  $C_\infty$  symmetry. Under these circumstances, chiral SFG is surface-sensitive.

When using chiral SFG to study biopolymers at interfaces, we and many other researchers use outputs from Ti:sapphire lasers as the visible beam in the near-infrared region at roughly 800 nm.<sup>20</sup> This wavelength is far away from electronic transitions of most biopolymers, which are in the ultraviolet region (e.g., protein at ~280 nm and DNA at ~260 nm),<sup>20, 31</sup> thus satisfying the condition of electronic non-resonance. However, in the cases when the visible beam used in an SFG experiment is in the visible range (e.g., the doubling of the Nd:YAG laser with an output at 532 nm) or when biopolymers contain prosthetic chromophores (e.g., retinal proteins) that absorb in the visible region (e.g., 400-600 nm), the resonance or pre-resonance effect can amplify the antisymmetric components of the Raman tensor and thereby enhance bulk chiral SFG signals. These enhanced bulk signals can potentially mix with the chiral SFG signal generated from a chiral interface, jeopardizing the surface sensitivity of chiral SFG. Nonetheless, the use of the 800-nm beam in studies of biopolymers without prosthetic chromophores meets the condition of electronic non-resonance.<sup>20, 36</sup> Therefore, chiral SFG is expected to be useful in probing biopolymers at interfaces and address many important problems, such as adsorbing protein on a polymer surface, detecting DNA using biosensor, and self-assembling biomolecules to make functional materials.

Guided by theory, our chiral SFG experiments and computations assess the orthogonal  $\chi_{zyx}^{(2)}$  elements. We obtain chiral SFG spectra by measuring  $\chi_{zyx}^{(2)}$  using the *psp* polarization setting (*p*-polarized SFG, *s*-polarized visible, and *p*-polarized infrared) (Figure 2a).<sup>20</sup> We simulate chiral SFG spectra by calculating  $\chi_{zyx}^{(2)}$  for direct comparison with experimental data. Combining

experimental and computational approaches, we are developing a framework of using chiral SFG for investigating vibrational structures and dynamics of biopolymers and their hydration at aqueous interfaces.<sup>3, 4</sup>

### Selectivity to Chiral Macroscopic Folding of Biopolymers

Since Simpson developed chiral SFG theory,<sup>15-17</sup> researchers have been using chiral SFG to study proteins and DNA at interfaces. Chen and coworkers reported the first chiral SFG spectrum of amide I modes of antiparallel  $\beta$ -sheets at interfaces.<sup>37</sup> Yet, without knowledge about the chiral SFG response from other protein secondary structures, there had been limited applications of chiral SFG for protein characterization. We studied a series of protein secondary structures at aqueous interfaces and obtained spectra of not only the amide I modes but also the N-H stretches of the protein backbone.<sup>19, 38, 39</sup> We found that different protein secondary structures give distinctive chiral SFG responses: disordered structures are silent for both the amide I and N-H stretching vibrational modes,  $\alpha$ -helical structures are only active for N-H stretching but not amide I, and  $\beta$ -sheet structures are active for both N-H stretching and amide I.<sup>18, 19</sup> The differences in selectivity of the same vibrational modes for various secondary structures is unprecedented in other vibrational tools (e.g., infrared, Raman, vibrational circular dichroism spectroscopy, etc.). This unique selectivity allows chiral SFG to simplify the deconvolution of vibrational spectra for studying protein secondary structures, which is a constant challenge in vibrational studies of proteins due to spectral overlap.<sup>40, 41</sup> Moreover, infrared studies of proteins often require D<sub>2</sub>O as solvent to suppress water background because the O-H bending modes ( $\sim 1600\text{ cm}^{-1}$ ) overlap with protein amide I modes, and the O-H stretches ( $\sim 3400\text{ cm}^{-1}$ ) overlap with protein N-H stretches. Chiral SFG does not require D<sub>2</sub>O because chiral SFG is sensitive only to chiral surfaces with C<sub>∞</sub> symmetry (Figure 2b) and is not sensitive to the majority of water molecules in the systems under study. We then applied chiral SFG to study amyloid aggregation on lipid surfaces,<sup>19, 38</sup> correlate orientations of protein aggregates at interfaces with disease mechanisms,<sup>42</sup> examine biological functions of a native surface-active protein,<sup>43</sup> and develop methods for probing proton exchange of proteins at interfaces.<sup>44</sup> Other researchers have also used chiral SFG to characterize protein structures, study ultrafast dynamics of proteins, and probe other amide modes at interfaces.<sup>31, 45-47</sup>

More recently, we used chiral SFG to demonstrate the crowding effect of protein folding at interfaces.<sup>1</sup> We designed a molecular construct by conjugating a lipid to a protein (Figure 3a). The lipid part anchors the construct at the air-water interface while the protein part is a zinc finger. The zinc finger exhibits  $\alpha$ -helical and disordered structures in the absence of zinc ions but folds into the  $\beta\beta\alpha$  structure comprising an antiparallel  $\beta$ -hairpin and an  $\alpha$ -helix upon binding to zinc ions. Because the  $\alpha$ -helical and disordered structures do not contribute to the amide I signals, chiral SFG can detect zinc-induced folding of the  $\beta$ -hairpin structures without background from the  $\alpha$ -helical and disordered structures (Figure 3b). This background-free detection makes the interpretation of chiral SFG spectra much simpler than that of achiral SFG spectra (Figure 3c). A comparison of Figures 3b and 3c shows that the chiral amide I signals can serve as binary readouts to report zinc finger folding (Figure 3b). Our study shows that steric repulsion can inhibit folding of zinc fingers at the interface, whereas releasing the steric repulsion by adding phospholipid as a spacer can restore the folding (Figure 3a), demonstrating the two-dimensional crowding effect on a protein folding at the interface.

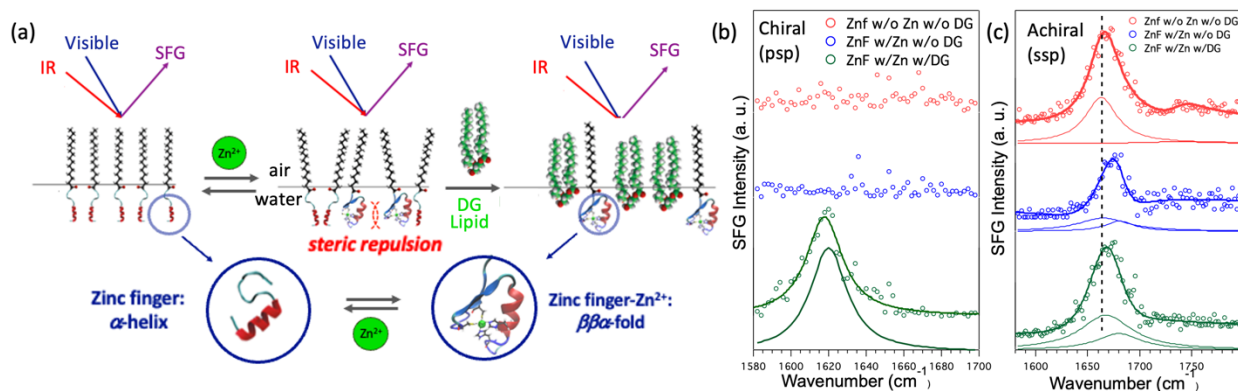


**Figure 3. Two-dimensional crowding effect on protein folding.** (a) Zinc finger covalently linked to palmitic acid for surface anchoring; zinc ion induces folding of the N-terminus from the disordered structure to the  $\beta$ -hairpin; 1,2-dipalmitoyl-sn-glycerol (DG) is used as a spacer to control the crowding at the air/water interface. (b) Chiral and achiral SFG spectra in the amide I region under three conditions: (i) without  $Zn^{2+}$  and without DG spacer lipid (red); (ii) with  $Zn^{2+}$  and without DG (blue), (iii) with  $Zn^{2+}$  and with DG (green). Adapted with permission from ref 1. Copyright 2018 the Royal Society of Chemistry.

Aside from proteins, chiral SFG can also probe DNA at interfaces. Geiger and coworkers reported C-H stretches of duplex DNA,<sup>48-50</sup> attributing a major vibrational band to methyl (CH<sub>3</sub>) stretches. However, Simpson's chiral SFG theory predicts that methyl groups with three-fold symmetry (C<sub>3v</sub>) cannot generate chiral SFG signals.<sup>16, 17, 32</sup> Looking into this discrepancy, we showed that intermolecular and/or intramolecular vibrational coupling can reduce symmetry, thereby breaking the C<sub>3v</sub> symmetry and making the methyl stretches chiral-SFG active.<sup>21</sup> We then studied C-H stretches from DNA duplexes at various interfaces.<sup>2</sup> We established three sample platforms for probing DNA at interfaces (Figure 4a). Different from previous studies, we probed the phase of the chiral SFG response and used single-stranded DNA as controls. With these strategies, we made several new observations.<sup>2</sup> First, chiral SFG is silent to single-stranded DNA but provides strong signals from double-stranded DNA (Figure 4b), offering simple binary readouts for sensing DNA hybridization. Second, the phase of chiral SFG spectra reverses when the DNA duplex is switched from the native (D-) to the non-native (L-) form (Figure 4c), indicating that chiral SFG can distinguish the absolute chirality of DNA duplexes. Third, chiral SFG captures the aromatic C-H stretching modes of nucleobases in the DNA duplex at >3000 cm<sup>-1</sup> whereas these modes are silent in the achiral SFG spectra (Figure 4b), demonstrating that chiral SFG can probe highly specific local structures for revealing DNA-drug interactions and DNA photodamage. Finally, chiral SFG detects C-H stretches not only from the canonical antiparallel DNA duplex but also from a non-canonical parallel duplex (Figure 4d), suggesting the promise of chiral SFG for characterizing DNA secondary structures. Overall, our results suggest that chiral SFG can be potentially useful to build high-throughput DNA sensors, probe various modes of drug binding to DNA, and beyond.

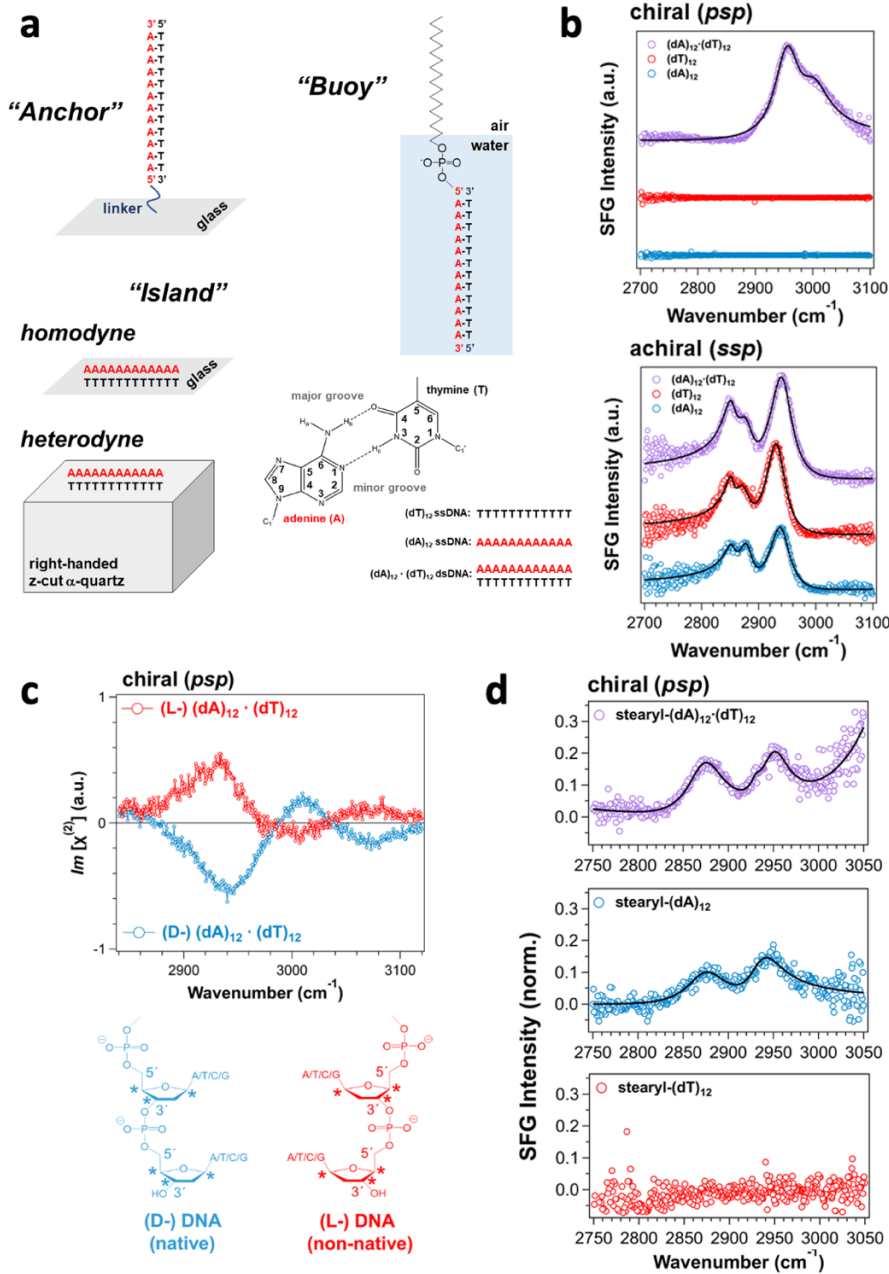
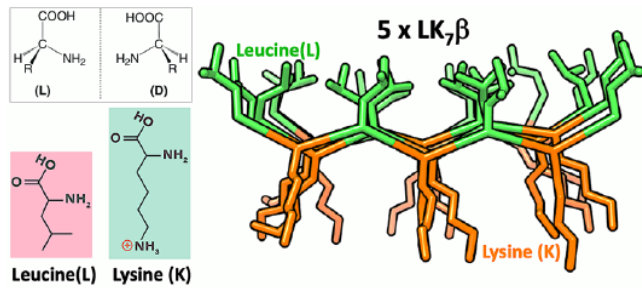


**Figure 4. Characterization of DNA at interfaces.** (a) Surface platforms for immobilizing DNA at the air-glass interface using a covalent linkage (anchor), at the air-glass or crystalline quartz interface (island), and at the air-water interface using a stearyl moiety (buoy). The structure of an adenine—thymine base pair. (b) Chiral (*psp*) and achiral (*ssp*) SFG spectra of single- and double-stranded DNA at the air-glass interface. (c) Heterodyne phase-resolved chiral SFG spectra of (L-) and (D-) (dA)<sub>12</sub> · (dT)<sub>12</sub> double-stranded DNA on quartz. Chemical structures of native (D-) DNA versus non-native (L-) DNA. (d) Chiral SFG spectra of stearyl-(dA)<sub>12</sub> · (dT)<sub>12</sub> double-stranded DNA, stearyl-(dA)<sub>12</sub>, and stearyl-(dT)<sub>12</sub> at the air-water interface. The chiral SFG signal of stearyl-(dA)<sub>12</sub> is due to a non-canonical parallel double helix of (dA)<sub>12</sub> · (dA)<sub>12</sub>. Adapted with permission with permission from ref 2. Copyright 2022 American Chemical Society.

## Selectivity to Hydration of Biopolymers at Interfaces

We have recently performed experiments and computations to investigate water structures in the hydration shell of a  $\beta$ -sheet protein at an interface.<sup>3, 4, 14, 21</sup> In 2017, Petersen and coworkers reported the chiral SFG signal from a double-helix DNA at a frequency around  $3200\text{ cm}^{-1}$  and attributed the signal to O-H stretches of water molecules embedded in the minor groove of DNA,<sup>51</sup> revealing the potential of chiral SFG to probe hydration structures of biomolecules at interfaces. Nonetheless, before using chiral SFG to solve any problem, we need to understand how it is possible for achiral water molecules to generate a chiral SFG response. Building on our experience of studying proteins, we asked whether we could observe chiral SFG signals of water hydrating proteins, and if yes, what part of the system generates the signals.

To address these questions, we examined a model peptide (LK<sub>7</sub> $\beta$ ) that forms antiparallel  $\beta$ -sheets at interfaces (Scheme 1).<sup>52</sup> We deposited the peptide on a glass surface and obtained chiral SFG spectra at around  $3200\text{ cm}^{-1}$ .<sup>14</sup> This spectral region encompasses protein N-H and water O-H signals. Thus, we must differentiate the water signals from the protein signals. Because only the water O-H stretches can be red-shifted by <sup>18</sup>O substitution, we used isotopically labeled H<sub>2</sub><sup>18</sup>O or D<sub>2</sub><sup>18</sup>O as solvent. We observed selected vibrational bands shifting to the red by around  $10\text{ cm}^{-1}$  (Figure 5), thus confirming chiral SFG signals from water (Figure 5).<sup>14</sup> Moreover, using heterodyne detection, we obtained phase-resolved chiral SFG spectra of LK<sub>7</sub> $\beta$  on a crystalline quartz surface.<sup>3</sup> When switching the protein chirality from the native (L-) to the non-native (D-) form, we observed flipping of the phase for not only the protein N-H stretches but also the water O-H stretches (Figure 6).<sup>3</sup> This observation has profound implications because not only biopolymers but also their hydration structures are chiral, raising a question about the role of water in the molecular evolution of biological homochirality, where native proteins are in the (L-) form and nucleic acids are in the (D-) form.



**Scheme 1.** Structure of antiparallel  $\beta$ -sheet LK<sub>7</sub> $\beta$  (LKLKLKL).

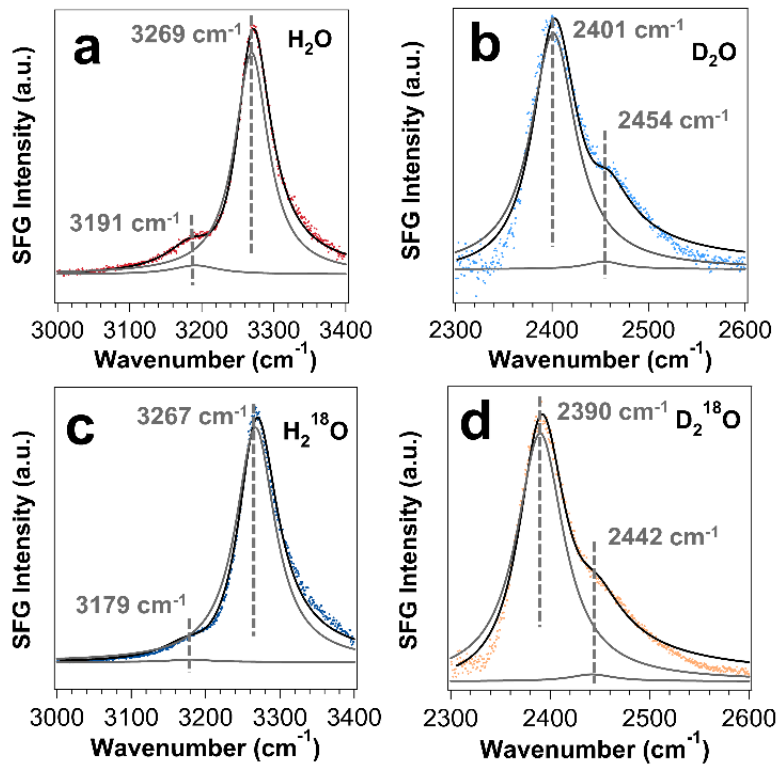


**Figure 5. Chiral SFG spectra of LK<sub>7</sub> $\beta$  deposited on glass slides.** The samples are prepared using solvents of (a) H<sub>2</sub>O, (b) D<sub>2</sub>O, (c) H<sub>2</sub><sup>18</sup>O, and (d) D<sub>2</sub><sup>18</sup>O. Each spectrum exhibits a minor and a major vibrational band. The <sup>18</sup>O substitution shifts the minor peak in the H<sub>2</sub>O spectrum and both major and minor peaks in the D<sub>2</sub>O spectrum by about 10 cm<sup>-1</sup>, confirming water contributions to the chiral SFG spectra. Adapted with permission from ref 14. Copyright 2019 American Chemical Society.

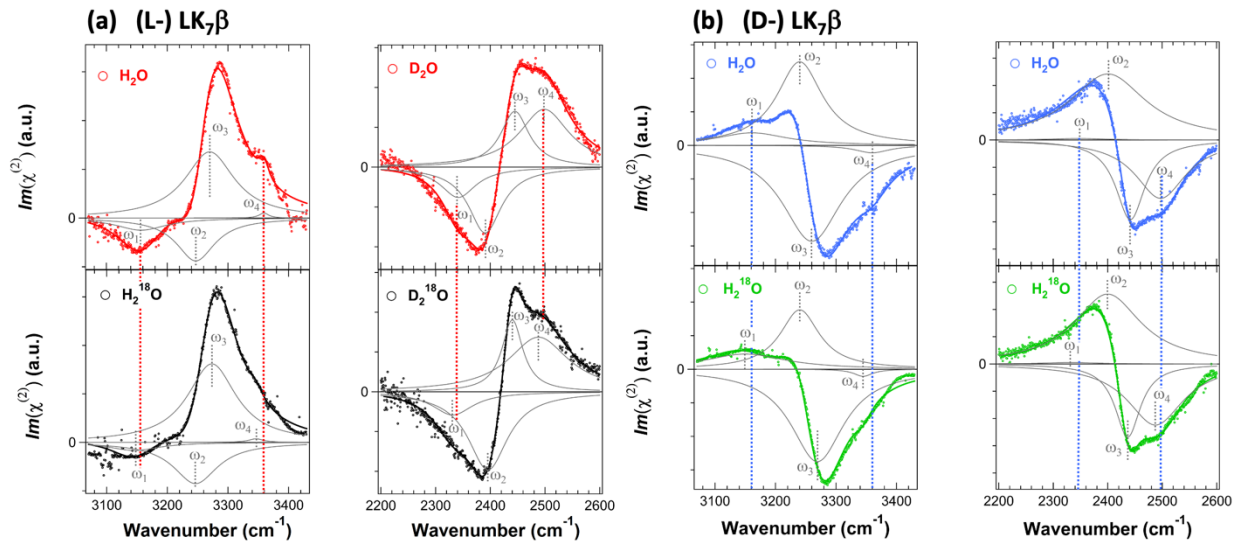


**Figure 6. Phase-resolved chiral SFG spectra of LK<sub>7</sub>β on quartz surface.** (a) (L-) LK<sub>7</sub>β and (b) (D-) LK<sub>7</sub>β. Chiral SFG spectra in the O-H/N-H region (~3200 cm<sup>-1</sup>) of LK<sub>7</sub>β prepared in H<sub>2</sub>O and H<sub>2</sub><sup>18</sup>O and chiral SFG spectra in the O-D/N-D region (~2400 cm<sup>-1</sup>) of LK<sub>7</sub>β prepared in D<sub>2</sub>O and D<sub>2</sub><sup>18</sup>O. All spectra are fit to Lorentzian lineshapes. Individual vibrational bands based on the fitting are shown in gray, and the sum of these peaks are shown in solid lines. Red or blue dashed lines indicate perturbation by <sup>18</sup>O substitution for the highest ( $\omega_1$ ) and lowest ( $\omega_4$ ) vibrational bands that are assigned to water O-H stretching. The two middle ( $\omega_2$  and  $\omega_3$ ) bands are not impacted by <sup>18</sup>O substitution and are assigned to protein N-H or N-D stretches. The parameters fitting the four spectra of (L-) LK<sub>7</sub>β are comparable to those of (D-) LK<sub>7</sub>β, except the phase of each vibrational band reverses. Adapted with permission from ref 3. Copyright 2020 National Academy of Science.

To understand our experimental results at the theoretical level, we computed the chiral SFG response of water around the β-sheet protein.<sup>3, 4</sup> Although chiral SFG signals of water were first reported from DNA,<sup>51</sup> simulation of the chiral SFG signals of water around any biomolecules had yet to be reported. We applied Skinner's electrostatic map<sup>53-55</sup> to simulate the chiral SFG spectra of water around the β-sheet protein, which is modeled by five peptide strands of LK<sub>7</sub>β in either the (L-) or (D-) forms at the vacuum-water interface (Figure 7a). Because these peptide strands are highly amphiphilic with hydrophobic leucine sidechains pointing up to the air phase and hydrophilic positively charged lysine sidechains pointing down to the aqueous phase, the orientation of this protein relative to the interface is highly restricted, making the β-sheet lie flat at the interface.<sup>56</sup> The simulated spectra show strong water O-H stretching bands, and the phase of these bands reverses with the protein chirality (Figure 7b), agreeing with experimental observations (Figures 6 and 7c).<sup>3, 4</sup> The combined computational and experimental studies (Figures 5-7) have established that chiral SFG signals of achiral water molecules originate from water

assembling around the protein into a chiral supramolecular structure with the chirality imprinted from the protein.

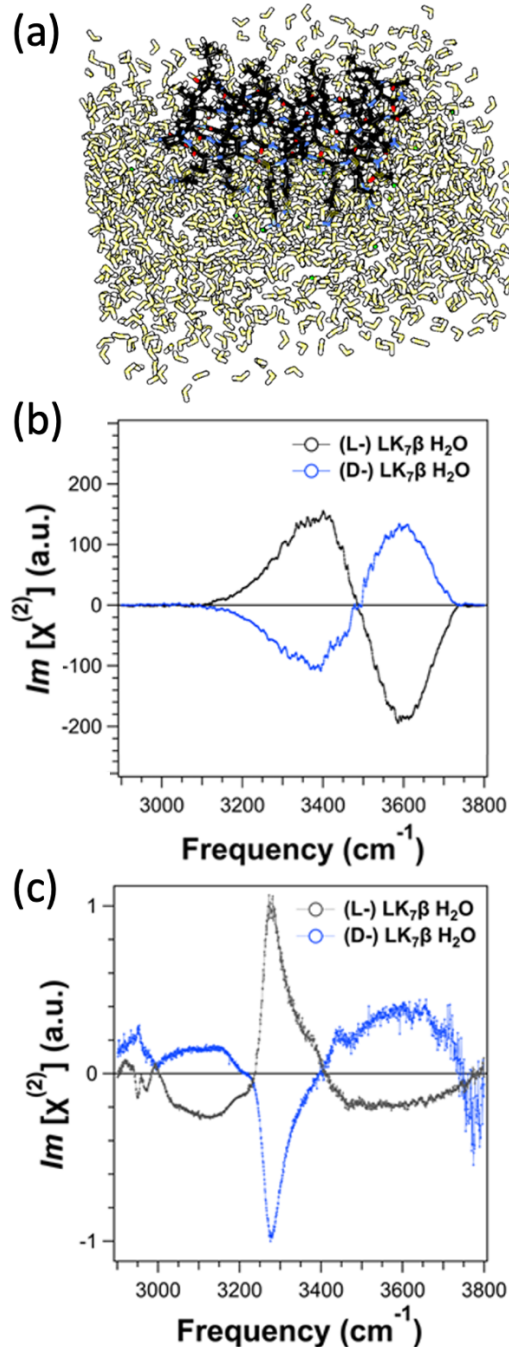


**Figure 7. Computational model and simulated chiral SFG spectra and comparison to experimental results.** (a) Molecular model for the simulation: an LK<sub>7</sub>β pentamer (black) at the vacuum-water interface forming an antiparallel β-sheet surrounded by water molecules (yellow).

(b) Simulated chiral SFG spectra of (L-)  $\text{LK}_7\beta$  and (D-)  $\text{LK}_7\beta$  comprising only the water O-H stretching responses. (c) Experimental heterodyne phase-resolved spectra in the N-H/O-H region of (L-)  $\text{LK}_7\beta$  and (D-)  $\text{LK}_7\beta$  showing signals with opposite signs. Adapted with permission from ref 4. Copyrights 2022 American Chemical Society.

Further computational analyses show that chiral SFG can probe vibrational structures of water hydrating the  $\beta$ -sheet protein at the air-water interface with selectivity to the first hydration shell.<sup>4</sup> Using a Voronoi tessellation algorithm, we identified immediate neighbors of the protein as water molecules in the first hydration shell and immediate neighbors of the first hydration shell as water molecules in the second hydration shell. We could then simulate chiral SFG spectra of the first and second hydration shells. The simulated spectra reveal that almost all (>92%) of the chiral SFG signal comes from the first hydration shell, and the signal from the second hydration shell drops to almost zero (Figure 8).

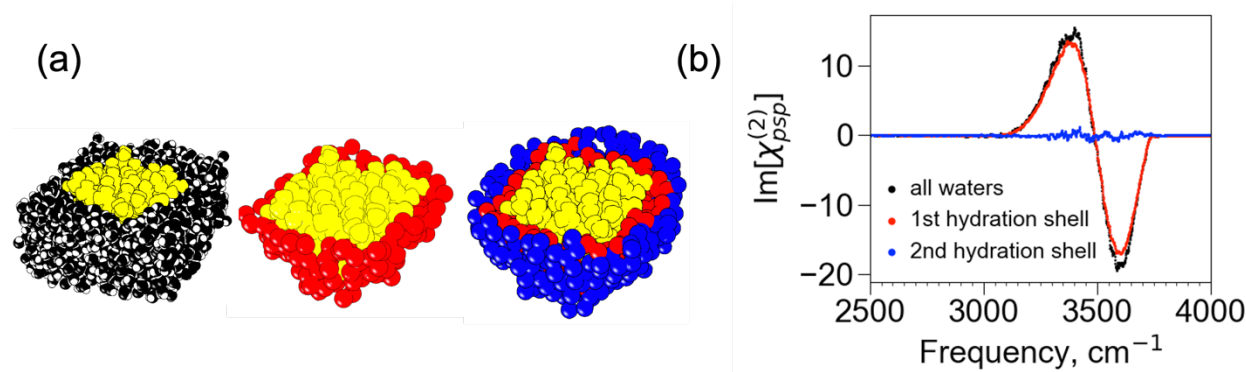


**Figure 8. Selectivity of first hydration shell.** (a) The model system contains the  $\text{LK}_7\beta$  protein (yellow) with all water (black), but the spectra can be computed from select subsets of water, such as only the first hydration shell (red) or only the second hydration shell (blue). (b) Calculated spectra of the O-H stretches from all water molecules (black), the first hydration shell (red), and the second hydration shell (blue). Adapted with permission from ref 4. Copyright 2022 American Chemical Society.

To understand the remarkable selectivity to the first hydration shell, we analyzed water dipoles around the  $\beta$ -sheet protein at the interface (Figure 9).<sup>4</sup> We found that water dipoles generally orient toward the protein because of the positively charged lysine residues. The organization outside the first hydration shell is quite symmetric (Figures 9a-c), giving rise to at least two reflection planes ( $\sigma_{//}$  and  $\sigma_{\perp}$ ) perpendicular to the interface. Hence, the organization of water molecules outside the first hydration shell is in  $\text{C}_{\infty v}$  symmetry and thus not chiral-SFG active

according to chiral SFG theory (see Figure 2b). Inside the first hydration shell, however, local interactions with the protein break the pattern of symmetry and remove the reflection planes (Figures 9d and 9e). Thus, water molecules inside the first hydration shell exhibit  $C_\infty$  symmetry, thereby generating chiral SFG signals. This analysis has established an intuitive but rigorous molecular explanation based on chiral SFG theory (Figure 2b) for the selectivity of chiral SFG to first hydration shell structures of proteins at interfaces.<sup>4</sup>

This work has developed a synergistic experimental and computational framework that can be further used to understand molecular structures and dynamics of water in hydration shells of biopolymers at interfaces.<sup>3, 4, 14, 21</sup> In this framework, experimental chiral SFG vibrational spectra can serve as quantitative benchmarks for validation of computational tools developed for predicting structural evolution and dynamics of water-biopolymer interactions at aqueous interfaces.

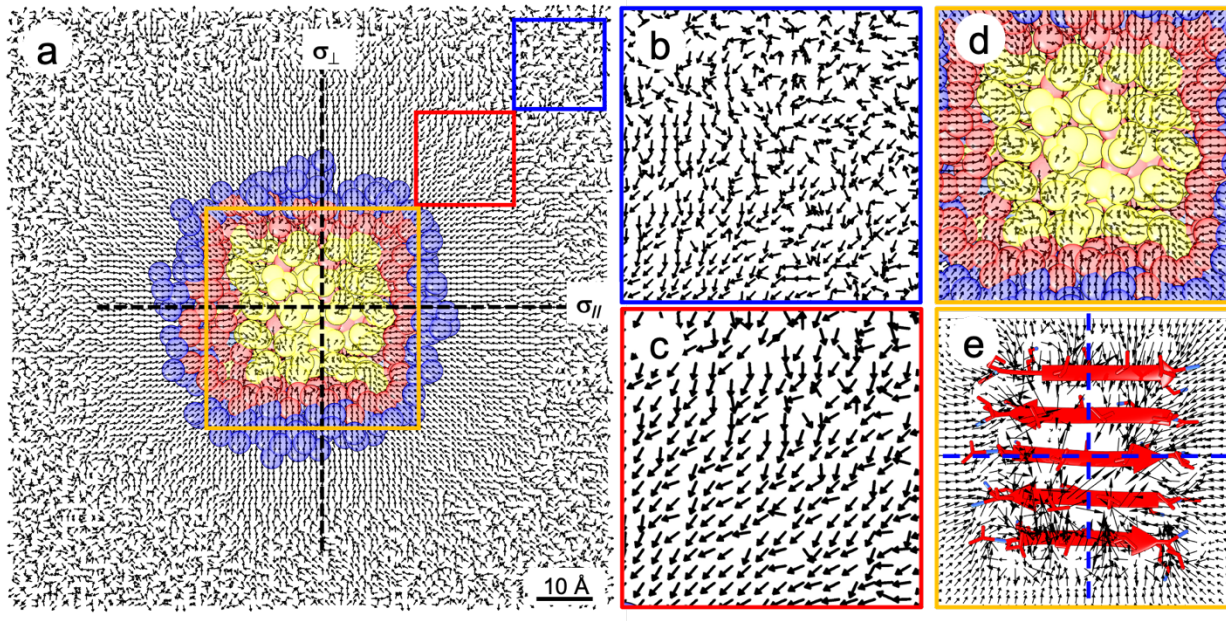


**Figure 9. Water dipole arrangements around LK7 $\beta$  at the vacuum-water interface.** (a) Top view of water dipoles at the vacuum-water interface. Each arrow is a unit vector of a water dipole averaged in a  $1\text{-}\text{\AA}^3$  grid box with protein (yellow), first hydration shell (red), and second hydration shell (blue). (b), (c), and (d) Zoomed-in details in the blue, red, and orange boxes. Water dipoles in panel (c) point toward LK7 $\beta$  due to the positively charged lysine residues. (e) Zoomed-in depiction of the orange box showing the magnitude of each water dipole. Water arrangement outside the first hydration shell constitutes at least two reflection planes ( $\sigma_{\parallel}$  and  $\sigma_{\perp}$ ) perpendicular to the interface, and thus the water molecules are arranged in  $C_{\infty v}$  symmetry. Water arrangement

within the first hydration shell is less symmetric without a reflection plane and thus has  $C_\infty$  symmetry. Therefore, chiral SFG theory (Figure 2b) implies that only water molecules in the first hydration shell are chiral-SFG active. Adapted with permission from ref 4. Copyright 2022 American Chemical Society.

## Conclusion and Outlook

Our recent experiments and computations have established unique selectivity of chiral SFG for probing the intricate interplay of chirality, water, and interfaces. This method can simultaneously differentiate (1) surface signals from bulk signals, (2) various secondary structures of biopolymers, and (3) water molecules in hydration shells of the biopolymers from water molecules elsewhere. Because chiral SFG offers surface-selectivity and works under ambient conditions for *in situ* and real-time studies, it can complement NMR, X-ray crystallography, neutron scattering, and terahertz spectroscopy in probing hydration structures of biomolecules. The unique selectivity of chiral SFG will allow it to address problems related to structure-function correlations of biomolecules at interfaces.

Nonetheless, there are still several remaining challenges. One of these challenges is the difficulty in interpreting water spectra due to the coupling of water O-H stretches with N-H stretches of biopolymers. To tackle this problem, our group developed an electrostatic-frequency map that allows for simulating N-H spectra of the protein backbone and thereby examining the effect of the vibrational coupling between the protein backbone and water.<sup>57</sup> We also need to develop new methods to simulate the N-H stretching response from nucleic acids. Another challenge is for spectroscopists to obtain high-quality biological samples and identify problems with genuine biological relevance, which can be most effectively overcome by collaboration with researchers in the biological and biomedical fields. In addition, to broaden the scope of applications, chiral SFG needs to be combined with advanced spectroscopic methods, such as pump-probe and multi-dimensional techniques. This method development will enable studies of ultrafast dynamics of important biomolecular events, such as photodamage of DNA, solvation dynamics of photoactive proteins, and intramolecular vibrational energy redistribution of biocatalysts.

Despite these challenges, our case study of the LK<sub>7</sub> $\beta$  protein at the air-water interface has produced an experimental and computational framework for investigating structural and

dynamical properties of biomolecules at aqueous interfaces. This framework can serve as the basis for future developments to elucidate biological functions at interfaces for attacking fundamental and engineering problems. The unique selectivity of chiral SFG should empower researchers to explore new chemistry emerging from the molecular interplay of chirality, water, and interfaces.

## Biographies

Elsa C. Y. Yan is a professor in the Chemistry Department at Yale University. She obtained her B.S. in Chemistry from the Chinese University of Hong Kong. Working with Kenneth Eisenthal at Columbia University, she developed second-order spectroscopy to probe colloidal surfaces. Then, she became a joint postdoctoral fellow with Richard Mathies at UC Berkeley and Thomas Sakmar at The Rockefeller University, exploring functional mechanism of transmembrane receptors. At Yale, she develops and applies optical spectroscopy to study biomolecular structures and functions. She focuses on fundamental studies using chiral SFG spectroscopy to probe chiral biomacromolecular structures and their hydration at interfaces.

Ethan A. Perets is a postdoctoral researcher at Harvard University working to develop novel technologies for neurobiological imaging. Ethan received his B.A. in biochemistry from Columbia University, his M.A. in the history of art from the Courtauld Institute of Art, and his Ph.D. in chemistry from Yale University. Working alongside Professors Elsa C. Y. Yan and Sharon Hammes-Schiffer at Yale, Ethan applied chiral sum frequency generation spectroscopy to study the interplay of secondary structure and hydration of proteins and DNA at molecular interfaces.

Daniel Konstantinovsky is a PhD student at Yale University working on modeling chiral sum frequency generation spectroscopy responses of proteins, nucleic acids, and the water around them with the goal of understanding the physics of the macromolecular solvation shell. Daniel received his B.S. in Chemistry from Haverford College and subsequently worked in Dr. Alexander Rudensky's group at Memorial Sloan Kettering, studying the effect of bile acids on

regulatory T cells, before turning to computational work at Yale as a joint student in the Hammes-Schiffer and Yan groups.

Sharon Hammes-Schiffer is a Sterling Professor of Chemistry at Yale University. She received her B.A. from Princeton University and her Ph.D. from Stanford University, followed by two years at AT&T Bell Laboratories. Her academic career progressed from the University of Notre Dame to Pennsylvania State University to the University of Illinois to Yale University. Her work encompasses the development of analytical theories and computational methods, as well as applications to a wide range of chemical, biological, and interfacial systems.

### **Acknowledgements**

This work was supported by the National Institutes of Health Grant R35GM139449 (S.H.-S.). The protein work was supported by the NSF Grant (CHE-2108690) (E.C.Y.Y.) and the DNA work was supported by the NSF Grant (CHE-1905169) (E.C.Y.Y.). D.K. was supported by these grants. E.A.P. was supported by the NIH (5T32GM008283-31) and a John C. Tully Chemistry Research Fellowship from Yale University.

### **References**

- (1) Liu, W.; Fu, L.; Wang, Z.; Sohrabpour, Z.; Li, X.; Liu, Y.; Wang, H.-f.; Yan, E. C. Y. Two dimensional crowding effects on protein folding at interfaces observed by chiral vibrational sum frequency generation spectroscopy. *Phys. Chem. Chem. Phys* **2018**, *20*, 22421-22426, 10.1039/C7CP07061F. DOI: 10.1039/C7CP07061F.
- (2) Perets, E. A.; Olesen, K. B.; Yan, E. C. Y. Chiral Sum Frequency Generation Spectroscopy Detects Double-Helix DNA at Interfaces. *Langmuir* **2022**, *38*, 5765-5778. DOI: 10.1021/acs.langmuir.2c00365.
- (3) Perets, E. A.; Konstantinovsky, D.; Fu, L.; Chen, J.; Wang, H.-F.; Hammes-Schiffer, S.; Yan, E. C. Y. Mirror-image antiparallel  $\beta$ -sheets organize water molecules into superstructures of opposite chirality. *Proc. Natl. Acad. Sci. U.S.A* **2020**, *117*, 32902-32909. DOI: 10.1073/pnas.2015567117 (acccesed 2022/09/21).
- (4) Konstantinovsky, D.; Perets, E. A.; Santiago, T.; Velarde, L.; Hammes-Schiffer, S.; Yan, E. C. Y. Detecting the First Hydration Shell Structure around Biomolecules at Interfaces. *ACS Cent. Sci.* **2022**, *8*, 1404-1414, DOI: 10.1021/acscentsci.2c00702.

(5) Soai, K.; Kawasaki, T.; Matsumoto, A. Asymmetric Autocatalysis of Pyrimidyl Alkanol and Its Application to the Study on the Origin of Homochirality. *Acc. Chem. Res.* **2014**, *47*, 3643-3654. DOI: 10.1021/ar5003208.

(6) Wang, Z. M.; Xu, W. L.; Liu, L.; Zhu, T. F. A synthetic molecular system capable of mirror-image genetic replication and transcription. *Nat. Chem.* **2016**, *8*, 698-704. DOI: 10.1038/NCHEM.2517.

(7) Milton, R. C. d.; Milton, S. C. F.; Kent, S. B. H. Total Chemical Synthesis of a D-Enzyme: The Enantiomers of HIV-1 Protease Show Reciprocal Chiral Substrate Specificity. *Science* **1992**, *256*, 1445-1448. DOI: doi:10.1126/science.1604320.

(8) Levy, Y.; Onuchic, J. N. Water mediation in protein folding and molecular recognition. *Annu. Rev. Biophys.* **2006**, *35*, 389-415. DOI: 10.1146/annurev.biophys.35.040405.102134.

(9) Ball, P. Water as an active constituent in cell biology. *Chem. Rev.* **2008**, *108*, 74-108. DOI: 10.1021/cr068037a.

(10) Nihonyanagi, S.; Yamaguchi, S.; Tahara, T. Direct evidence for orientational flip-flop of water molecules at charged interfaces: A heterodyne-detected vibrational sum frequency generation study. *J. Chem. Phys.* **2009**, *130*, 204704. DOI: 10.1063/1.3135147.

(11) Sovago, M.; Campen, R. K.; Bakker, H. J.; Bonn, M. Hydrogen bonding strength of interfacial water determined with surface sum-frequency generation. *Chem. Phys. Lett.* **2009**, *470*, 7-12. DOI: 10.1016/j.cplett.2009.01.009.

(12) Shen, Y. R.; Ostroverkhov, V. Sum-Frequency Vibrational Spectroscopy on Water Interfaces: Polar Orientation of Water Molecules at Interfaces. *Chem. Rev.* **2006**, *106*, 1140-1154. DOI: 10.1021/cr040377d.

(13) Stiopkin, I. V.; Weeraman, C.; Pieniazek, P. A.; Shalhout, F. Y.; Skinner, J. L.; Benderskii, A. V. Hydrogen bonding at the water surface revealed by isotopic dilution spectroscopy. *Nature* **2011**, *474*, 192-195, Article. DOI: 10.1038/nature10173.

(14) Perets, E. A.; Yan, E. C. Y. Chiral Water Superstructures around Antiparallel beta-Sheets Observed by Chiral Vibrational Sum Frequency Generation Spectroscopy. *J. Phys. Chem. Lett.* **2019**, *10*, 3395-3401, Article. DOI: 10.1021/acs.jpclett.9b00878.

(15) Perry, J. M.; Moad, A. J.; Begue, N. J.; Wampler, R. D.; Simpson, G. J. Electronic and vibrational second-order nonlinear optical properties of protein secondary structural motifs. *J. Phys. Chem. B* **2005**, *109*, 20009-20026. DOI: 10.1021/jp0506888.

(16) Moad, A. J.; Simpson, G. J. A Unified Treatment of Selection Rules and Symmetry Relations for Sum-Frequency and Second Harmonic Spectroscopies. *J. Phys. Chem. B* **2004**, *108*, 3548-3562. DOI: 10.1021/jp035362i.

(17) Simpson, G. J. Molecular Origins of the Remarkable Chiral Sensitivity of Second-Order Nonlinear Optics. *ChemPhysChem* **2004**, *5*, 1301-1310. DOI: 10.1002/cphc.200300959.

(18) Fu, L.; Wang, Z.; Yan, E. C. Y. Chiral vibrational structures of proteins at interfaces probed by sum frequency generation spectroscopy. *Int. J. Mol. Sci.* **2011**, *12*, 9404-9425.

(19) Fu, L.; Liu, J.; Yan, E. C. Y. Chiral sum frequency generation spectroscopy for characterizing protein secondary structures at interfaces. *J. Am. Chem. Soc.* **2011**, *133*, 8094-8097.

(20) Yan, E. C.; Fu, L.; Wang, Z.; Liu, W. Biological macromolecules at interfaces probed by chiral vibrational sum frequency generation spectroscopy. *Chem. Rev.* **2014**, *114*, 8471-8498.

(21) Konstantinovsky, D.; Perets, E. A.; Yan, E. C. Y.; Hammes-Schiffer, S. Simulation of the Chiral Sum Frequency Generation Response of Supramolecular Structures Requires Vibrational Couplings. *J. Phys. Chem. B* **2021**, *125*, 12072-12081. DOI: 10.1021/acs.jpcb.1c06360.

(22) Shen, Y. Surface properties probed by second-harmonic and sum-frequency generation. *Nature* **1989**, *337*, 519-525.

(23) Shen, Y.-R. *The Principles of Nonlinear Optics*; Wiley-Interscience, 1984.

(24) Richmond, G. Molecular bonding and interactions at aqueous surfaces as probed by vibrational sum frequency spectroscopy. *Chem. Rev.* **2002**, *102*, 2693-2724.

(25) Eisenthal, K. B. Liquid Interfaces Probed by Second-Harmonic and Sum-Frequency Spectroscopy. *Chem. Rev.* **1996**, *96*, 1343-1360. DOI: 10.1021/cr9502211.

(26) Morita, A. Theory of Sum Frequency Generation Spectroscopy. In *Theory of Sum Frequency Generation Spectroscopy*, Vol. 97; 2018; pp 1-264.

(27) Bredenbeck, J.; Ghosh, A.; Nienhuys, H.-K.; Bonn, M. Interface-Specific Ultrafast Two-Dimensional Vibrational Spectroscopy. *Acc. Chem. Res.* **2009**, *42*, 1332-1342. DOI: 10.1021/ar900016c.

(28) Nihonyanagi, S.; Mondal, J. A.; Yamaguchi, S.; Tahara, T. Structure and Dynamics of Interfacial Water Studied by Heterodyne-Detected Vibrational Sum-Frequency Generation. In *Annu. Rev. Phys. Chem.*, Vol 64, Johnson, M. A., Martinez, T. J. Eds.; Annual Review of Physical Chemistry, Vol. 64; Annual Reviews, 2013; pp 579-603.

(29) Wang, H.-F.; Gan, W.; Lu, R.; Rao, Y.; Wu, B.-H. Quantitative spectral and orientational analysis in surface sum frequency generation vibrational spectroscopy (SFG-VS). *Int. Rev. Phys. Chem.* **2005**, *24*, 191-256. DOI: 10.1080/01442350500225894.

(30) Chen, Z.; Shen, Y. R.; Somorjai, G. A. Studies of polymer surfaces by sum frequency generation vibrational spectroscopy. *Annu. Rev. Phys. Chem.* **2002**, *53*, 437-465. DOI: 10.1146/annurev.physchem.53.091801.115126.

(31) Hosseinpour, S.; Roeters, S. J.; Bonn, M.; Peukert, W.; Woutersen, S.; Weidner, T. Structure and Dynamics of Interfacial Peptides and Proteins from Vibrational Sum-Frequency Generation Spectroscopy. *Chem. Rev.* **2020**, *120*, 3420-3465, Review. DOI: 10.1021/acs.chemrev.9b00410.

(32) Simpson, G. J. *Nonlinear Optical Polarization Analysis in Chemistry and Biology*; Cambridge University Press, 2017. DOI: DOI: 10.1017/9781139019026.

(33) Belkin, M. A.; Kulakov, T. A.; Ernst, K. H.; Yan, L.; Shen, Y. R. Sum-frequency vibrational spectroscopy on chiral liquids: A novel technique to probe molecular chirality. *Phys. Rev. Lett.* **2000**, *85*, 4474-4477. DOI: 10.1103/PhysRevLett.85.4474.

(34) Belkin, M. A.; Han, S. H.; Wei, X.; Shen, Y. R. Sum-frequency generation in chiral liquids near electronic resonance. *Phys. Rev. Lett.* **2001**, *87*. DOI: 10.1103/PhysRevLett.87.113001.

(35) Liu, F. Antisymmetric nonresonant vibrational Raman scattering. *J. Phys. Chem.* **1991**, *95*, 7180-7185. DOI: 10.1021/j100172a017.

(36) Yan, E. C. Y.; Wang, Z.; Fu, L. Proteins at Interfaces Probed by Chiral Vibrational Sum Frequency Generation Spectroscopy. *J. Phys. Chem. B* **2015**, *119*, 2769-2785.

(37) Wang, J.; Chen, X. Y.; Clarke, M. L.; Chen, Z. Detection of chiral sum frequency generation vibrational spectra of proteins and peptides at interfaces in situ. *Proc Natl Acad Sci U S A* **2005**, *102*, 4978-4983. DOI: 10.1073/pnas.0501206102.

(38) Fu, L.; Ma, G.; Yan, E. C. Y. In situ misfolding of human islet amyloid polypeptide at interfaces probed by vibrational sum frequency generation. *J. Am. Chem. Soc.* **2010**, *132*, 5405-5412.

(39) Fu, L.; Wang, Z.; Yan, E. C. Y. N-H Stretching Modes Around 3300 Wavenumber From Peptide Backbones Observed by Chiral Sum Frequency Generation Vibrational Spectroscopy. *Chirality* **2014**, *26*, 521-524. DOI: 10.1002/chir.22306.

(40) Barth, A. Infrared spectroscopy of proteins. *Biochim. Biophys. Acta. Bioenerg.* **2007**, *1767*, 1073-1101, Review. DOI: 10.1016/j.bbabi.2007.06.004.

(41) Tamm, L. K.; Tatulian, S. A. Infrared spectroscopy of proteins and peptides in lipid bilayers. *Q. Rev. Biophys.* **1997**, *30*, 365-429. DOI: undefined From Cambridge University Press Cambridge Core.

(42) Xiao, D.; Fu, L.; Liu, J.; Batista, V. S.; Yan, E. C. Y. Amphiphilic Adsorption of Human Islet Amyloid Polypeptide Aggregates to Lipid/Aqueous Interfaces. *J. Mol. Biol.* **2012**, *421*, 537-547. DOI: <https://doi.org/10.1016/j.jmb.2011.12.035>.

(43) Wang, Z.; Morales-Acosta, M. D.; Li, S. H.; Liu, W.; Kanai, T.; Liu, Y. T.; Chen, Y. N.; Walker, F. J.; Ahn, C. H.; Leblanc, R. M.; Yan, E. C. Y. A narrow amide I vibrational band observed by sum frequency generation spectroscopy reveals highly ordered structures of a biofilm protein at the air/water interface. *Chem. Commun.* **2016**, *52*, 2956-2959, Article. DOI: 10.1039/c5cc05743d.

(44) Fu, L.; Xiao, D.; Wang, Z.; Batista, V. S.; Yan, E. C. Y. Chiral sum frequency generation for in situ probing proton exchange in antiparallel  $\beta$ -sheets at interfaces. *J. Am. Chem. Soc.* **2013**, *135*, 3592-3598.

(45) Tan, J. J.; Luo, Y.; Ye, S. J. A Highly Sensitive Femtosecond Time-Resolved Sum Frequency Generation Vibrational Spectroscopy System with Simultaneous Measurement of Multiple Polarization Combinations. *Chinese J. Chem. Phys.* **2017**, *30*, 671-677. DOI: 10.1063/1674-0068/30/cjcp1706114.

(46) Tan, J.; Zhang, J.; Luo, Y.; Ye, S. Misfolding of a Human Islet Amyloid Polypeptide at the Lipid Membrane Populates through  $\beta$ -Sheet Conformers without Involving  $\alpha$ -Helical Intermediates. *J. Am. Chem. Soc.* **2019**, *141*, 1941-1948. DOI: 10.1021/jacs.8b08537.

(47) Engel, M. F. M.; VandenAkker, C. C.; Schleeger, M.; Velikov, K. P.; Koenderink, G. H.; Bonn, M. The Polyphenol EGCG Inhibits Amyloid Formation Less Efficiently at Phospholipid Interfaces than in Bulk Solution. *J. Am. Chem. Soc.* **2012**, *134*, 14781-14788. DOI: 10.1021/ja3031664.

(48) Boman, F. C.; Gibbs-Davis, J. M.; Heckman, L. M.; Stepp, B. R.; Nguyen, S. T.; Geiger, F. M. DNA at Aqueous/Solid Interfaces: Chirality-Based Detection via Second Harmonic Generation Activity. *J. Am. Chem. Soc.* **2009**, *131*, 844-848. DOI: 10.1021/ja808007b.

(49) Stokes, G. Y.; Gibbs-Davis, J. M.; Boman, F. C.; Stepp, B. R.; Condie, A. G.; Nguyen, S. T.; Geiger, F. M. Making “Sense” of DNA. *J. Am. Chem. Soc.* **2007**, *129*, 7492-7493. DOI: 10.1021/ja071848r.

(50) Walter, S. R.; Geiger, F. M. DNA on Stage: Showcasing Oligonucleotides at Surfaces and Interfaces with Second Harmonic and Vibrational Sum Frequency Generation. *J. Phys. Chem. Lett.* **2010**, *1*, 9-15. DOI: 10.1021/jz9001086.

(51) McDermott, M. L.; Vanselous, H.; Corcelli, S. A.; Petersen, P. B. DNA’s Chiral Spine of Hydration. *ACS Cent. Sci.* **2017**, *3*, 708-714. DOI: 10.1021/acscentsci.7b00100.

(52) DeGrado, W. F.; Lear, J. D. Induction of peptide conformation at apolar water interfaces. 1. A study with model peptides of defined hydrophobic periodicity. *J. Am. Chem. Soc.* **1985**, *107*, 7684-7689. DOI: 10.1021/ja00311a076.

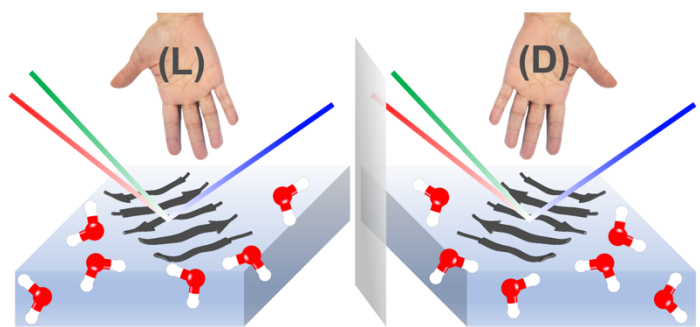
(53) Corcelli, S. A.; Lawrence, C. P.; Skinner, J. L. Combined electronic structure/molecular dynamics approach for ultrafast infrared spectroscopy of dilute HOD in liquid H<sub>2</sub>O and D<sub>2</sub>O. *J. Chem. Phys.* **2004**, *120*, 8107-8117. DOI: 10.1063/1.1683072.

(54) Auer, B. M.; Skinner, J. L. IR and Raman spectra of liquid water: Theory and interpretation. *J. Chem. Phys.* **2008**, *128*, 224511. DOI: 10.1063/1.2925258.

(55) Pieniazek, P. A.; Tainter, C. J.; Skinner, J. L. Interpretation of the water surface vibrational sum-frequency spectrum. *J. Chem. Phys.* **2011**, *135*, 044701, research-article. DOI: A11.04.0161R.

(56) Perets, E. A.; Videla, P. E.; Yan, E. C. Y.; Batista, V. S. Chiral Inversion of Amino Acids in Antiparallel beta-Sheets at Interfaces Probed by Vibrational Sum Frequency Generation Spectroscopy. *J. Phys. Chem. B* **2019**, *123*, 5769-5781, Article. DOI: 10.1021/acs.jpcb.9b04029.

(57) Konstantinovsky, D.; Perets, E. A.; Santiago, T.; Olesen, K.; Wang, Z.; Soudackov, A. V.; Yan, E. C. Y.; Hammes-Schiffer, S. Design of an Electrostatic Frequency Map for the NH Stretch of the Protein Backbone and Application to Chiral Sum Frequency Generation Spectroscopy. *J. Phys. Chem. B* **2023**, *127*, 2418-2429. DOI: 10.1021/acs.jpcb.3c00217.



**TOC graphic.**